

# Discovery of interstellar mercapto radicals (SH) with the GREAT instrument on SOFIA

D. A. Neufeld<sup>1</sup>, E. Falgarone<sup>2</sup>, M. Gerin<sup>2</sup>, B. Godard<sup>3</sup>, E. Herbst<sup>4</sup>, G. Pineau des Forêts<sup>2,5</sup>, A. I. Vasyunin<sup>4</sup>, R. Güsten<sup>6</sup>,  
H. Wiesemeyer<sup>6</sup>, and O. Ricken<sup>6,7</sup>

<sup>1</sup> The Johns Hopkins University, 3400 North Charles St. Baltimore, MD 21218, USA

<sup>2</sup> LERMA, CNRS UMR 8112, École Normale Supérieure & Observatoire de Paris, Paris, France

<sup>3</sup> Departamento de Astrofísica, Centro de Astrobiología, CSIC-INTA, Torrejón de Ardoz, Madrid, Spain

<sup>4</sup> Department of Chemistry, University of Virginia, McCormick Road, P.O. Box 400319, Charlottesville, VA 22904, USA

<sup>5</sup> Institut d'Astrophysique Spatiale, CNRS UMR 8617, Université Paris-Sud, Orsay, France

<sup>6</sup> Max-Planck-Institut für Radioastronomie, Auf dem Hügel 69, 53121 Bonn, Germany

<sup>7</sup> I. Physikalisches Institut der Universität zu Köln, Zùlpicher Strasse 77, 50937 Köln, Germany

Preprint online version: September 26, 2018

## ABSTRACT

We report the discovery of interstellar mercapto radicals along the sight-line to the submillimeter continuum source W49N. We have used the GREAT instrument on SOFIA to observe the 1383 GHz  ${}^2\Pi_{3/2} J = 5/2 \leftarrow 3/2$  lambda doublet in the upper sideband of the L1 receiver. The resultant spectrum reveals SH absorption in material local to W49N, as well as in foreground gas, unassociated with W49N, that is located along the sight-line. For the foreground material at velocities in the range 37 – 44 km/s with respect to the local standard of rest, we infer a total SH column density  $\sim 4.6 \times 10^{12} \text{ cm}^{-2}$ , corresponding to an abundance of  $\sim 7 \times 10^{-9}$  relative to  $\text{H}_2$ , and yielding an SH/ $\text{H}_2\text{S}$  abundance ratio  $\sim 0.13$ . The observed SH/ $\text{H}_2\text{S}$  abundance ratio is much smaller than that predicted by standard models for the production of SH and  $\text{H}_2\text{S}$  in turbulent dissipation regions and shocks, and suggests that the endothermic neutral-neutral reaction  $\text{SH} + \text{H}_2 \rightarrow \text{H}_2\text{S} + \text{H}$  must be enhanced along with the ion-neutral reactions believed to produce  $\text{CH}^+$  and  $\text{SH}^+$  in diffuse molecular clouds.

**Key words.** Astrochemistry – ISM: molecules – Submillimeter: ISM – Molecular processes – ISM: clouds

## 1. Introduction

In the seven decades following the discovery of interstellar CH (Swings & Rosenfeld 1937) – the first identified interstellar molecule – five or six additional neutral diatomic hydrides have been discovered in the interstellar gas: OH (Weinreb 1963),  $\text{H}_2$  (Carruthers 1970), HCl (Blake et al. 1985), NH (Meyer & Roth 1991), HF (Neufeld et al. 1995), and SiH (Schilke et al. 2001; a tentative detection). These discoveries were obtained from observations over a remarkably wide range of wavelengths, from the far-ultraviolet ( $\text{H}_2$ , discovered at 1013 - 1110 Å), through the near-UV (NH at 3358 Å), the optical (CH at 4300 Å), the far-infrared (HF at 122  $\mu\text{m}$ ), the submillimeter (SiH at 478  $\mu\text{m}$ , and HCl at 479  $\mu\text{m}$ ), and the radio (OH at 18 cm) spectral regions. In addition to these neutral molecules, four hydride molecular ions have now been discovered:  $\text{CH}^+$  (Douglas & Herzberg 1941),  $\text{OH}^+$  (Gerin et al. 2010a; Wyrowski et al. 2010),  $\text{SH}^+$  (Benz et al. 2010), and  $\text{HCl}^+$  (DeLuca et al. 2012; Gupta et al. 2012), the latter three in just the past two years.

The diatomic hydrides represent the simplest of interstellar molecules, and – carefully interpreted in the context of astrochemical models – may provide key information about the interstellar environment. For example, the  $\text{OH}^+$  abundance yields constraints upon the rate of cosmic ray ionization, which initiates the chemical network leading to  $\text{OH}^+$  (e.g. Neufeld et al. 2010). The  $\text{CH}^+$ ,  $\text{SH}^+$  and OH abundances, by contrast, probe the influence of shocks and turbulent dissipation, which heat the interstellar gas and/or lead to ambipolar diffusion; these processes may thereby drive endothermic chemical reactions that lead to

enhanced abundances of  $\text{CH}^+$ ,  $\text{SH}^+$  and OH (e.g. Flower, Pineau des Forêts, & Hartquist 1985; Godard, Falgarone & Pineau des Forêts 2009)

The mercapto radical, SH – which, like  $\text{CH}^+$  and  $\text{SH}^+$ , is expected to show a strong abundance enhancement in warm regions that are heated by shocks or turbulent dissipation – has been conspicuously absent from the list of previously-detected molecules. In its ground rotational state, SH can absorb radiation in the  ${}^2\Pi_{3/2} J = 5/2 \leftarrow 3/2$  lambda doublet near 1383 GHz, a frequency that is completely inaccessible from the ground, due to atmospheric absorption, and which – by bad fortune – falls right in the gap between Bands 5 and 6 of the *Herschel Space Observatory*'s Heterodyne Instrument for the Far-Infrared (HIFI). Fortunately, this spectral region is now accessible to the GREAT (German Receiver for Astronomy at Terahertz Frequencies) instrument<sup>1</sup> on SOFIA (the Stratospheric Observatory for Infrared Astronomy), and in this *Letter* we report the first detection of interstellar SH with the use of that instrument. The observations and data reduction are described in §2, and the results presented in §3. In §4 we discuss the implications of the measured SH column density in the context of astrochemical models.

<sup>1</sup> GREAT is a development by the MPI für Radioastronomie and the KOSMA / Universität zu Köln, in cooperation with the MPI für Sonnensystemforschung and the DLR Institut für Planetenforschung.

**Table 1.**  ${}^2\Pi_{3/2} J = 5/2 \leftarrow 3/2$  SH lines observed with GREAT

Transition	Frequency (GHz)	$A_{ij}$ ( $s^{-1}$ )	$\Delta v$ ( $km\ s^{-1}$ )
$F = 2^+ \leftarrow 2^-$	1382.9056	$0.47 \times 10^{-3}$	+0.98
$F = 3^+ \leftarrow 2^-$	1382.9101	$4.72 \times 10^{-3}$	
$F = 2^+ \leftarrow 1^-$	1382.9168	$4.24 \times 10^{-3}$	-1.45
$F = 2^- \leftarrow 2^+$	1383.2365	$0.47 \times 10^{-3}$	+1.02
$F = 3^- \leftarrow 2^+$	1383.2412	$4.72 \times 10^{-3}$	
$F = 2^- \leftarrow 1^+$	1383.2478	$4.24 \times 10^{-3}$	-1.43

<sup>(a)</sup> Velocity shift relative to the strongest hyperfine component of the respective doublet

## 2. Observations and data reduction

We observed the  ${}^2\Pi_{3/2} J = 5/2 \leftarrow 3/2$  transition of SH, a lambda doublet for which the strongest hyperfine components ( $F = 3 \leftarrow 2$ ) lie at frequencies of 1382.910 and 1383.241 GHz, in the upper sideband of the L1 receiver. A broad atmospheric ozone feature is present in the lower sideband, at a frequency of 1379.50 GHz. The LO settings were selected to separate this feature as far as possible (in IF frequency) from the target SH transition. These observations, with a combined on-source integration time of 4.0 min, were carried out on 2011 September 28th as part of the SOFIA Basic Science Program. The telescope beam, of diameter  $\sim 21''$  HPBW, was centered on W49N at  $\alpha = 19h\ 10m\ 13.2s$ ,  $\delta = +09^{\circ}06'12.0''$  (J2000). The observations were performed in dual beam switch mode, with a chopper frequency of 1 Hz and the reference positions located  $75''$  on either side of the source along an East-West axis. The AFTS backend provided 8192 spectral channels at a spacing of 183.1 kHz. Thanks to laboratory spectroscopy performed by Morino & Kawaguchi (1995) and by Klisch et al. (1996), the SH rest frequencies are known to estimated accuracy of  $< 2$  MHz. The separation of the lambda doublet corresponds to a velocity shift of  $71.8\ km\ s^{-1}$ , and each doublet member is further split into three hyperfine components; the rest frequencies and spontaneous radiative rates are listed in Table 1, for an assumed SH dipole moment of 0.758 D (Meerts & Dynamus 1975).

The raw data were calibrated to the  $T_A^*$  (“forward beam brightness temperature”) scale, fitting independently the dry and the wet content of the atmospheric emission. Here, the assumed forward efficiency was 0.95 and the assumed beam efficiency for the L1 band was 0.54. The uncertainty in the flux calibration is estimated to be  $\sim 20\%$  (Heyminck et al. 2012). Additional data reduction – performed using CLASS<sup>2</sup> – entailed second-order baseline removal, averaging the data (with a weighting inversely proportional to the square of the r.m.s. noise), and spectral smoothing to a 3.7 MHz channel spacing.

In addition to the SOFIA observations of SH that are the primary subject of this Letter, we have carried out ancillary observations of the  $1_{10} - 1_{01}$  168.763 GHz transition of  $H_2S$ , using the IRAM 30 m telescope located in Pico Veleta near Granada (Spain) in December 2006 under good weather conditions. We used the C150 receiver, tuned in single side band, coupled to two spectrometers: the high resolution correlator VESPA with 40 kHz spectral resolution, and a broad band filter bank with 1 MHz spectral resolution. The data were acquired using the wobbler with a frequency of 0.5 Hz, for a total time of 32 minutes, and analyzed with the CLASS software.

<sup>2</sup> Continuum and Line Analysis Single-dish Software – <http://www.iram.fr/IRAMFR/GILDAS>

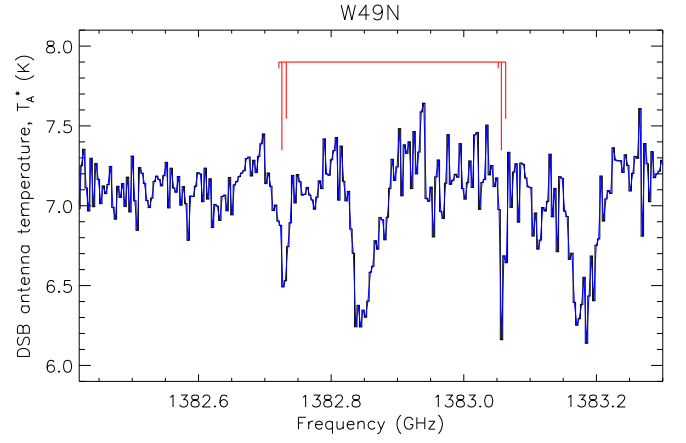


**Fig. 1.** Spectrum of SH  ${}^2\Pi_{3/2} J = 5/2 \leftarrow 3/2$  obtained by GREAT toward W49N. Note that because GREAT employs double sideband receivers, the complete absorption of radiation at a single frequency will reduce the measured antenna temperature to one-half the apparent continuum level. The lambda doubling and hyperfine splittings are indicated by the red bars for a component at an LSR velocity of  $40\ km\ s^{-1}$ .

## 3. Results

Figure 1 shows the observed spectrum of SH  ${}^2\Pi_{3/2} J = 5/2 \leftarrow 3/2$ , with the frequency scale corrected to the Local Standard of Rest (LSR). The double sideband continuum antenna temperature is  $T_A^*(cont) = 7.2\ K$ , and the r.m.s noise is 0.12 K in a 3.7 MHz channel. Because GREAT employs double sideband receivers, the complete absorption of radiation at a single frequency will reduce the measured antenna temperature to one-half the apparent continuum level.

In Figure 2, the fractional transmission is shown separately for each of the lambda doublets (top two panels), with the frequency scale expressed as Doppler velocities relative to the Local Standard of Rest (LSR) for the strongest hyperfine component of each doublet member. The transmission is given by  $2T_A^*/T_A^*(cont) - 1$ , given the assumption that the sideband gain ratio is unity. Analogous spectra are shown for the  $1_{10} - 1_{01}$  (ground state) transition of ortho- $H_2S$ , and for the  ${}^2\Pi_{3/2} J = 3/2^- \leftarrow {}^2\Pi_{1/2} J = 1/2^+$  transition of CH (Gerin et al. 2010b), believed to be a good tracer of  $H_2$  (e.g. Sheffer et al. 2008).

Absorption by SH is clearly detected in the range  $v_{LSR} \sim 5 - 20\ km\ s^{-1}$ , near the systemic velocity of the source. In addition, a narrow absorption feature is detected unequivocally near  $v_{LSR} \sim 39\ km\ s^{-1}$ , a component that is clearly present in the spectra of CH,  $H_2S$ , and many other molecules (e.g. Godard et al. 2010; Sonnentrucker et al. 2010). This component arises in a foreground cloud unassociated with W49N, which has an (kinematically-) estimated Galactocentric distance of  $\sim 6.7\ kpc$  (Godard et al. 2012).

In contrast to the case of CH, there is an absence of strong SH or  $H_2S$  absorption in the  $60 - 65\ km\ s^{-1}$  range. This behavior is similar to that observed for CS (Miyawaki, Hasegawa & Hayashi 1988) and for the nitrogen hydrides NH,  $NH_2$ , and  $NH_3$  (Persson et al. 2012); it may suggest that those molecules – such as SH – for which the  $v_{LSR} \sim 39\ km\ s^{-1}$  absorption is much stronger than that in the  $60 - 65\ km\ s^{-1}$  range all originate in material with a larger molecular fraction.

Because of its large spontaneous radiative decay rate ( $4.7 \times 10^{-3}\ s^{-1}$ ), the SH transition we have observed possesses a high

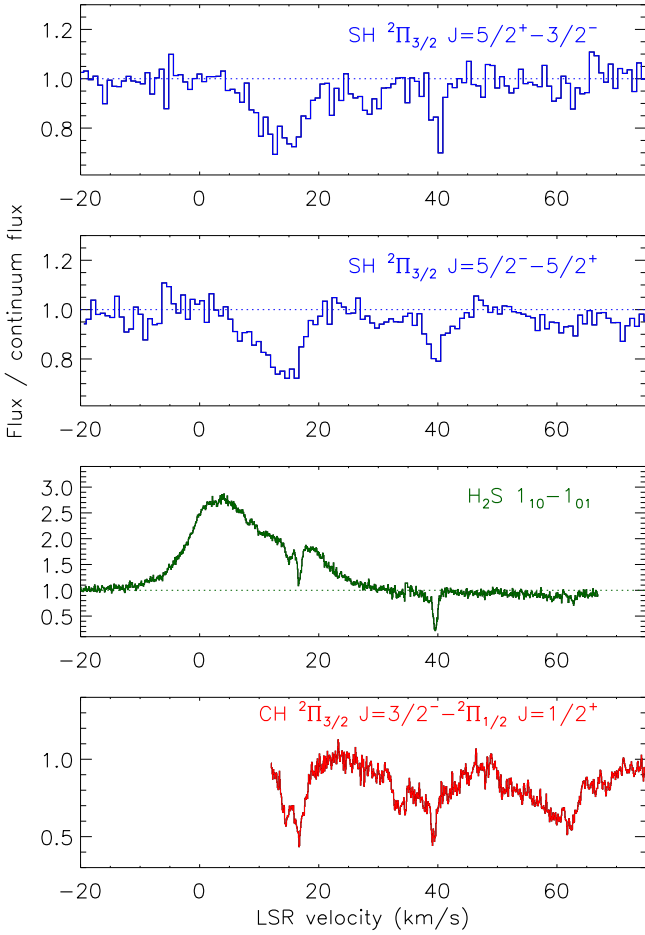


**Fig. 2.** Ratio of flux to continuum flux, for SH ( ${}^2\Pi_{3/2} J = 5/2 \leftarrow 3/2$ ), ortho- $\text{H}_2\text{S}$  ( $1_{10} \leftarrow 1_{01}$ ), and CH ( ${}^2\Pi_{3/2} J = 3/2^- \leftarrow {}^2\Pi_{1/2} J = 1/2^+$ ). The CH spectrum has been hyperfine-deconvolved.

critical density<sup>3</sup> ( $\gtrsim 10^7 \text{ cm}^{-3}$ , for an assumed collisional deexcitation rate  $\sim 10^{-10} \text{ cm}^3 \text{ s}^{-1}$ , similar to that computed by Offer et al. 1994 for the analogous transition of OH). Thus, in the foreground material unassociated with W49N, we expect that SH will be almost entirely in its ground rotational state,  ${}^2\Pi_{3/2} J = 3/2$ . In that case, the absorption optical depth, integrated over velocity and summed over the six components listed in Table 1, is given by

$$\int \tau dv = 2.88 \times 10^{-14} N(\text{SH}) \text{ cm}^2 \text{ km s}^{-1}. \quad (1)$$

(For the 5 - 20  $\text{km s}^{-1}$  velocity interval, equation (1) would likely yield an underestimate of the SH column density, because – for gas associated with the dense W49N cloud itself – there is likely to be a significant SH population in excited rotational states.)

In the present study<sup>4</sup>, we confine our attention to the narrow absorption feature appearing near  $v_{\text{LSR}} = 39 \text{ km s}^{-1}$ . In Table 2, we present estimates of the SH column density in the

<sup>3</sup> Here, “critical density” is defined as the gas density at which the collisional deexcitation rate equals the spontaneous radiative decay rate.

<sup>4</sup> A future study, requiring detailed modeling of the excitation of SH in W49N, will be needed to obtain an estimate of the  $\text{SH}^+$  column density in the source itself.

**Table 2.** Column densities for  $v_{\text{LSR}}$  in the 37 – 44  $\text{km s}^{-1}$  range

Molecule	Column density ( $\text{cm}^{-2}$ )	Abundance <sup>a</sup> relative to $\text{H}_2$	
SH	$4.6 \times 10^{12}$	$6.9 \times 10^{-9}$	Present work
ortho- $\text{H}_2\text{S}$	$2.6 \times 10^{13}$	$3.9 \times 10^{-8}$	Present work
$\text{SH}^+$	$2.6 \times 10^{12}$	$3.9 \times 10^{-9}$	Godard et al. 2012
para- $\text{H}_2\text{O}$	$1.5 \times 10^{13}$	$2.3 \times 10^{-8}$	Sonnentrucker et al. 2010
CH	$5.8 \times 10^{13}$	$9.0 \times 10^{-8}$	Gerin et al. 2012

<sup>(a)</sup> For an assumed  $\text{H}_2$  column of  $6.6 \times 10^{20} \text{ cm}^{-2}$  (Gerin et al. 2012)

39  $\text{km s}^{-1}$  absorbing cloud, along with analogous results obtained for ortho- $\text{H}_2\text{S}$  from IRAM 30m observations and for  $\text{SH}^+$ , para- $\text{H}_2\text{O}$  and CH from *Herschel*/HIFI observations. Given an estimated  $\text{H}_2$  column density of  $6.6 \times 10^{20} \text{ cm}^{-2}$  for this cloud (Godard et al. 2012), the observed SH column density implies an  $\text{SH}/\text{H}_2$  abundance ratio  $\sim 7 \times 10^{-9}$ , corresponding to  $\sim 0.003\%$  of the solar abundance of elemental sulfur. The  $\text{SH}/\text{SH}^+$  ratio is  $\sim 1.8$ . For an assumed  $\text{H}_2\text{S}$  ortho-to-para of 3 (the value expected in equilibrium), the  $\text{SH}/\text{H}_2\text{S}$  ratio is 0.13, a value that is significantly smaller than the  $\text{OH}/\text{H}_2\text{O}$  ratio  $\sim 1.0$  observed by SOFIA for this absorbing cloud (Wiesemeyer et al. 2012)

## 4. Discussion

Sulfur is unusual among the abundant elements in having a set of hydrides and hydride cations with relatively small bond energies. Thus *none* of the species S, SH,  $\text{S}^+$ ,  $\text{SH}^+$ , or  $\text{H}_2\text{S}^+$  can undergo an exothermic H atom abstraction reaction with  $\text{H}_2$ . (In other words,  $\text{X} + \text{H}_2 \rightarrow \text{XH} + \text{H}$  is endothermic for  $\text{X} = \text{S}, \text{SH}, \text{S}^+, \text{SH}^+$ , or  $\text{H}_2\text{S}^+$ .) Figure 3 illustrates the thermochemistry of the sulphur bearing hydrides by displaying the heats of formation of various sulphur-bearing species (with associated hydrogen atoms and  $\text{H}_2$  molecules involved in their formation.) The endothermicities of the reactions  $\text{X} + \text{H}_2 \rightarrow \text{XH} + \text{H}$ , expressed in temperature units,  $\Delta E/k$ , are 9641, 6984, 10117, 7634, and 4096 K respectively for  $\text{X} = \text{S}, \text{SH}, \text{S}^+, \text{SH}^+$ , and  $\text{H}_2\text{S}^+$ .

Clearly, these H atom abstraction reactions leading to the formation of the sulfur-containing hydrides are negligibly slow at the temperatures ( $< 100 \text{ K}$ ) typical of diffuse or dense molecular clouds. Nevertheless, surprisingly high column densities of  $\text{H}_2\text{S}$  have previously been observed in both diffuse molecular clouds and dense regions of active star-formation. For example, based on observations of diffuse foreground material along the sightlines to Sgr B2 (M) and W49N, Tieftrunk et al. (1994) measured  $\text{H}_2\text{S}$  abundances (of several  $\times 10^{-9}$  relative to  $\text{H}_2$  that were considerably larger than those predicted in standard chemical models. They suggested that  $\text{H}_2\text{S}$  might have been enhanced by high temperature reactions in shocks (e.g. Pineau des Forêts, Roueff, & Flower 1986) or by hydrogenation reactions on grain surfaces. Some smaller  $\text{H}_2\text{S}$  abundances (of several times  $10^{-10}$ ) were observed in diffuse clouds at high Galactic latitude by Lucas & Liszt (2002), while even larger  $\text{H}_2\text{S}$  abundances (up to  $\sim 10^{-6}$ ) have been inferred for dense regions of active star-formation (Minh et al. 1991).

More recently, enhanced  $\text{SH}^+$  abundances  $\sim \text{few} \times 10^{-9}$  have been measured in the diffuse ISM, using APEX (Menten et al. 2011) and *Herschel*/HIFI (Godard et al. 2012). These measurements have been interpreted as resulting from an increased reaction rate for  $\text{S}^+ + \text{H}_2 \rightarrow \text{SH}^+ + \text{H}$  in turbulent dissipation regions where the gas temperature is elevated and significant ion-neutral drift is present. The small  $\text{SH}/\text{H}_2\text{S}$  abundance ratio  $\sim 0.13$  inferred in §3 above for the 39  $\text{km s}^{-1}$  absorbing cloud suggests

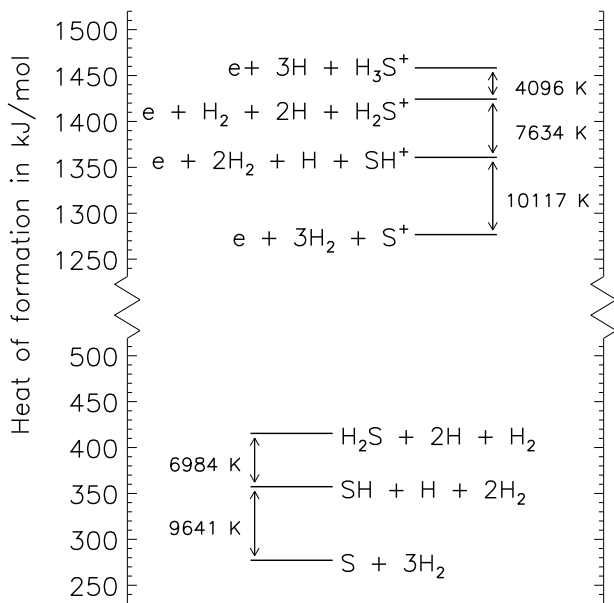


**Fig. 3.** Heats of formation of various S-bearing species (with associated H atoms produced during their formation), based upon thermochemical data from the NIST Chemistry Web book.

that the reaction  $SH + H_2 \rightarrow H_2S + H$  must be similarly increased, and argues that endothermic neutral-neutral reactions are enhanced along with ion-neutral reactions. As described below, this conclusion is supported by detailed modeling of (1) standard photodissociation regions (PDRs); (2) turbulent dissipation regions (TDRs); and (3) 'C'- and 'J'-type shock waves.

With the use of the Meudon PDR model (Le Petit et al. 2006), we have found that standard PDR models – i.e. models that do not include ion-neutral drift or additional heating mechanisms beyond those associated with ultraviolet irradiation and cosmic rays – greatly overpredict the SH/H<sub>2</sub>S ratio in low density diffuse gas, yielding typical values of 10<sup>4</sup>, and greatly underpredict the SH/H<sub>2</sub> and H<sub>2</sub>S/H<sub>2</sub> ratios. We found that SH/H<sub>2</sub>S ratios as small as unity are predicted only in gas clouds with densities,  $n_H$ , larger than 10<sup>4</sup> cm<sup>-3</sup>, and visual extinctions,  $A_V$  larger than 4, values that are both unreasonably large for the 39 km s<sup>-1</sup> absorbing cloud toward W49N. We have also investigated PDR models that include the effects of grain surface hydrogenation of S and SH and the subsequent photodesorption of H<sub>2</sub>S (Vasyunin & Herbst 2011); these too underpredict the SH/H<sub>2</sub> and H<sub>2</sub>S/H<sub>2</sub> ratios, unless an unreasonable large gas density is assumed. Using models for the chemistry of sulfur-bearing molecules in TDRs (Godard et al. 2009) and 'C'- and 'J'-type shocks (Pineau des Forêts et al. 1986), we determined that the predicted SH/H<sub>2</sub>S ratios in diffuse molecular clouds are ~ 10, significantly smaller than those for standard PDRs models without grain surface reactions, but nevertheless a factor ~ 100 larger than what is observed. Here, the production of SH is enhanced by the sequence  $S^+(H_2, H)SH^+(H_2, H)H_2S^+(e, H)SH$ , in which the first two endothermic reactions are significantly enhanced by ion-neutral drift. While the predicted SH and SH<sup>+</sup> abundances are broadly consistent with the observations, H<sub>2</sub>S is underpredicted by a factor of 100. As in the PDR models, smaller SH/H<sub>2</sub>S abundances are only predicted in clouds with implausibly large  $n_H$  and  $A_V$ . Apparently, standard models for PDRs, TDRs, or 'C'- or 'J'-type shocks cannot account for the

observed SH/H<sub>2</sub>S ratio, because they fail to predict a sufficient enhancement in the rates of neutral-neutral reactions.

We note however that existing models for sulfur chemistry in TDRs and 'C'-type shocks assume that all neutral species share a common velocity. As originally pointed out by Flower & Pineau des Forêts (1998) in the context of CH and CH<sup>+</sup> chemistry, neutral molecules that are produced by dissociative recombination of molecular ions in environments where there is significant ion-neutral drift – such as S and SH in the case of present interest – initially carry an imprint of the velocity of the ionized parents from which they formed. This effect may enhance endothermic reactions with H<sub>2</sub> that occur before the newly-formed neutral species has undergone sufficient elastic collisions to acquire the velocity of the neutral fluid. Detailed modeling, which we defer to a future publication, will be needed to determine whether the SH/H<sub>2</sub>S ratio serves as a diagnostic of this effect.

*Acknowledgements.* Based on observations made with the NASA/DLR Stratospheric Observatory for Infrared Astronomy. SOFIA Science Mission Operations are conducted jointly by the Universities Space Research Association, Inc., under NASA contract NAS2-97001, and the Deutsches SOFIA Institut under DLR contract 50 OK 0901. This research was supported by USRA through a grant for Basic Science Program 81-0014. EF, MG and BG acknowledge support from the French CNRS/INSU Programme PCMI (Physique et Chimie du Milieu Interstellaire).

## References

- Asplund, M., Grevesse, N., Sauval, A. J., Scott, P. 2009, *ARA&A*, 47, 481.  
 Benz, A. O., Bruderer, S., van Dishoeck, E. F., et al. 2010, *A&A*, 521, L35  
 Blake, G. A., Keene, J., & Phillips, T. G. 1985, *ApJ*, 295, 501  
 Carruthers, G. R. 1970, *ApJ*, 161, L81  
 Douglas, A. E., & Herzberg, G. 1941, *ApJ*, 94, 381  
 DeLuca et al. 2012, *ApJ*, submitted  
 Flower, D. R., Pineau des Forêts, G., & Hartquist, T. W. 1985, *MNRAS*, 216, 775  
 Flower, D. R., & Pineau des Forêts, G. 1998, *MNRAS*, 297, 1182  
 Gerin, M., de Luca, M., Black, J., et al. 2010a, *A&A*, 518, L110  
 Gerin, M., de Luca, M., Goicoechea, J. R., et al. 2010b, *A&A*, 521, L16  
 Gerin, M. et al. 2012, *A&A*, in preparation  
 Godard, B., Falgarone, E., Gerin, M., et al. 2012, *A&A*, in press  
 Godard, B., Falgarone, E., Gerin, M., Hily-Blant, P., & De Luca, M. 2010, *A&A*, 520, A20+  
 Godard, B., Falgarone, E., & Pineau Des Forêts, G. 2009, *A&A*, 495, 847  
 Gupta, H. et al. 2012, *ApJ*, in preparation  
 Heyminck, S., Graf, U. U., Güsten, R. et al. 2012, *A&A*, this volume  
 Klisch, E., Klaus, T., Belov, S. P., et al. 1996, *ApJ*, 473, 1118  
 Le Petit, F., Nehmé, C., Le Bourlot, J., & Roueff, E. 2006, *ApJS*, 164, 506  
 Lucas, R., & Liszt, H. S. 2002, *A&A*, 384, 1054  
 Meerts, W. L., & Dymanus, A. 1975, *Can J. Phys.* 53, 2123  
 Menten, K. M., Wyrowski, F., Belloche, A., et al. 2011, *A&A*, 525, A77+  
 Meyer, D. M., & Roth, K. C. 1991, *ApJ*, 376, L49  
 Miyawaki, R., Hasegawa, T., & Hayashi, M. 1988, *PASJ*, 40, 69  
 Minh, Y. C., Ziurys, L. M., Irvine, W. M., & McGonagle, D. 1991, *ApJ*, 366, 192  
 Morino, I., and Kawaguchi, K. 1995, *J. Mol. Spectrosc.*, 170, 172  
 Neufeld, D. A., Zmuidzinas, J., Schilke, P., & Phillips, T. G. 1997, *ApJ*, 488, L141  
 Neufeld, D. A., Goicoechea, J. R., Sonnentrucker, P., et al. 2010, *A&A*, 521, L10  
 Offer, A. R., van Hemert, M. C., & van Dishoeck, E. F. 1994, *J. Chem. Phys.*, 100, 362  
 Pineau des Forêts, G., Roueff, E., & Flower, D. R. 1986, *MNRAS*, 223, 743  
 Schilke, P., Benford, D. J., Hunter, T. R., Lis, D. C., & Phillips, T. G. 2001, *ApJS*, 132, 281  
 Sheffer, Y., Rogers, M., Federman, S. R., et al. 2008, *ApJ*, 687, 1075  
 Sonnentrucker, P., Neufeld, D. A., Phillips, T. G., et al. 2010, *A&A*, 521, L12  
 Swings, P., & Rosenfeld, L. 1937, *ApJ*, 86, 483  
 Tieftrunk, A., Pineau des Forêts, G., Schilke, P., & Walmsley, C. M. 1994, *A&A*, 289, 579  
 Vasyunin, A. I., & Herbst, E. 2011, in *The Molecular Universe*, Proceedings of the 280th Symposium of the International Astronomical Union held in Toledo, Spain, May 30-June 3, 2011  
 Weinreb, S. 1963, *Nature*, 200, 829  
 Wiesemeyer, H. et al. 2012, *A&A*, this volume  
 Wyrowski, F., Menten, K. M., Güsten, R., & Belloche, A. 2010, *A&A*, 518, A26